Human myelin proteome and comparative analysis with mouse myelin

Akihiro Ishii[a], Ranjan Dutta[b], Greg M. Wark[a], Sun-Il Hwang[c], David K. Han[c], Bruce D. Trapp[b], Steven E. Pfeiffer[a], and Rashmi Bansal[a,1]

Departments of [a]Neuroscience and [c]Cell Biology and Center for Vascular Biology, University of Connecticut Medical School, Farmington, CT, 06030; and [b]Department of Neurosciences, Lerner Research Institute, Cleveland Clinic, Cleveland, OH 44195

Myelin, formed by oligodendrocytes (OLs) in the CNS, is critical for axonal functions, and its damage leads to debilitating neurological disorders such as multiple sclerosis. Understanding the molecular mechanisms of myelination and the pathogenesis of human myelin disease has been limited partly by the relative lack of identification and functional characterization of the repertoire of human myelin proteins. Here, we present a large-scale analysis of the myelin proteome, using the shotgun approach of 1-dimensional PAGE and liquid chromatography/tandem MS. Three hundred eight proteins were commonly identified from human and mouse myelin fractions. Comparative microarray analysis of human white and gray matter showed that transcripts of several of these were elevated in OL-rich white matter compared with gray matter, providing confidence in their detection in myelin. Comparison with other databases showed that 111 of the identified proteins/transcripts also were expressed in OLs, rather than in astrocytes or neurons. Comparison with 4 previous myelin proteomes further confirmed more than 50% of the identified proteins and revealed the presence of 163 additional proteins. A select group of identified proteins also were verified by immunoblotting. We classified the identified proteins into biological subgroups and discussed their relevance in myelin biogenesis and maintenance. Taken together, the study provides insights into the complexity of this metabolically active membrane and creates a valuable resource for future in-depth study of specific proteins in myelin with relevance to human demyelinating diseases.

microarray | oligodendrocyte | proteomics | mass spectrometry

Myelin is a biologically active multilamellar membrane that is formed by oligodendrocytes (OLs) in the CNS and ensheathes axons. Communication between myelin and axons is critical for axonal functions, including rapid nerve conduction, survival, and cytoskeletal organization (1). The loss or damage of the myelin sheath results in serious neurological diseases such as multiple sclerosis. In addition, defects in myelin are correlated with schizophrenia (2) and age-dependent decline in brain function (3).

To prevent or ameliorate diseases of myelin, it is essential to understand the mechanism of its biogenesis and maintenance, which requires the identification and functional characterization of all myelin proteins—that is, the myelin proteome. Taylor et al. (4) reported the first rodent myelin proteome, and several studies then expanded it (5–7). Each study identified some additional proteins and others that were identified in previous proteomic studies, suggesting that no single identification method could successfully identify all myelin proteins. Nevertheless, these studies highlighted the complexity of myelin in rodents, which commonly are used as models for human disease. However, to apply this knowledge to diseases of human myelin, it is essential to establish a human myelin proteome and compare it with that in rodents.

Here, we present a large-scale undertaking that combines proteomics of human and mouse myelin and microarray analysis of human white and gray matter. It brings together information

from multiple sources, including the extensive transcriptome database of Cahoy et al. (8), to provide the field with a comprehensive picture of the numerous proteins not only of human myelin but also of those whose transcripts are enriched in human CNS white matter over gray matter and in purified rodent OLs over astrocytes and neurons, providing increased confidence in their identification in myelin. Performing human and mouse myelin proteomic analyses in parallel has allowed us to present at least 308 target proteins that are definitively present in myelin fractions of both species; thus, an investigation of them in mice clearly will be relevant for human studies. Further, a comparison of all the proteins that have been identified in 4 previous proteomes (4–7) has provided the identity of 163 additional proteins, many of which previously were unrecognized as being components of myelin. Based on our comprehensive analysis, we have short-listed 64 potentially interesting proteins for future in-depth analysis and, as an example, demonstrated by immunoblot analysis that 8 of these proteins are indeed reproducibly present in multiple human myelin samples. These analyses provide a valuable foundation and database for future studies to understand the functional implications of the presence of these proteins in normal human myelin and in the pathology of human myelin diseases.

Results and Discussion

Characterization of Human Myelin Samples for Proteomic Analysis. Myelin was purified from whole mouse brain and from multiple smaller sections of human brain from 4 subjects [supporting information (SI) Fig. S1]. Because these brain sections varied in their yield of myelin as a result of differences in their white matter content, we first asked if myelin that was purified from these sections using sucrose density gradient fractionation (see *Materials and Methods*) was similar with respect to its content of myelin proteins. Therefore, levels of major myelin proteins [2′, 3′-cyclic-nucleotide 3′-phosphodiesterase (CNP), myelin-associated glycoprotein (MAG), myelin basic protein (MBP), myelin OL glycoprotein (MOG) and OL-specific protein (OSP), myelin proteolipid protein (PLP)] were examined in 11 different samples from 4 human subjects through immunoblotting of the "main band fraction" of myelin (Fig. 1*A*). Each myelin sample showed similar intensities of signal, suggesting similar contents of myelin proteins in these samples.

It has been noted in rodents that myelin purification by sucrose density gradient centrifugation enriches compact myelin proteins in the lowest-density main band fraction, whereas axolemmal proteins are enriched in the high-density "pellet fraction" (9). To examine if this holds true for human myelin and to

A

Subject (sex, age)	1 (F, 53)				2 (M, 65)				3 (M, 53)	4 (F, 65)	
Sample	a	b	c	d	a	b	c	d	_	a	b
Yield (%)	8.0	9.8	22.3	8.5	17.7	12.9	21.0	11.3	41.6*	26.8	5.2*
CNP											
MAG											
MOG											
MBP											
OSP											
PLP											

B

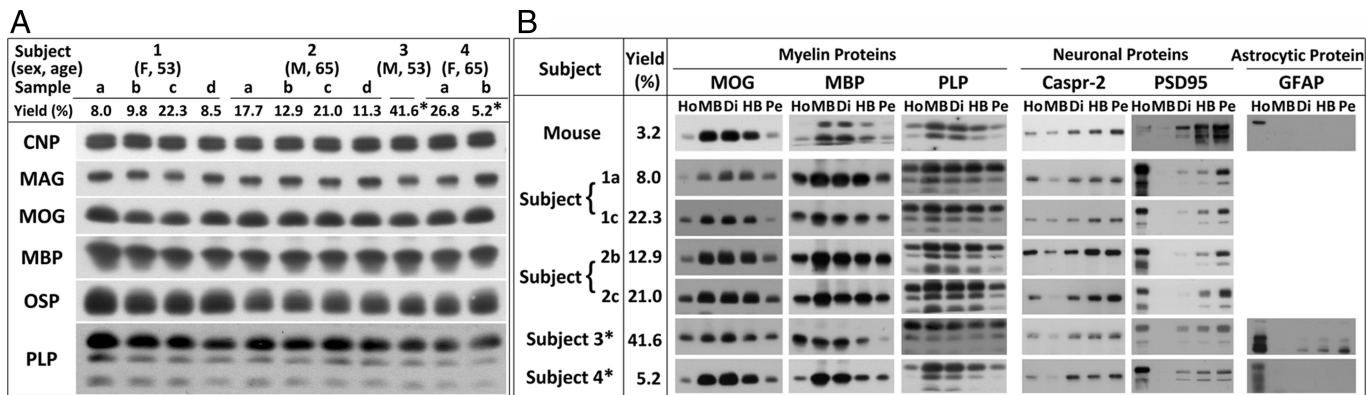| Subject	Yield (%)	Myelin Proteins			Neuronal Proteins		Astrocytic Protein
		MOG	MBP	PLP	Caspr-2	PSD95	GFAP
		Ho MB Di HB Pe	Ho MB Di HB Pe	Ho MB Di HB Pe	Ho MB Di HB Pe	Ho MB Di HB Pe	Ho MB Di HB Pe
Mouse	3.2						
Subject 1a	8.0						
Subject 1c	22.3						
Subject 2b	12.9						
Subject 2c	21.0						
Subject 3*	41.6						
Subject 4*	5.2						

Fig. 1. Characterization of human myelin samples for proteomic analysis. (*A*) Myelin was purified from 11 sections of normal human brain, obtained from different subjects (Fig. S1). Yield (%) is based on the amount of myelin protein (main band fraction) obtained from the total protein present in the starting brain homogenate. Equal amounts of proteins (5 μg) from main band myelin fractions were analyzed by immunoblotting for 6 specific major myelin proteins (CNP, MAG, MOG, MBP, OSP, and PLP). Note that each myelin sample showed similar intensities of signal, suggesting similar contents of myelin proteins in these samples. (*B*) Homogenate (Ho), prepared from 6 samples of normal human brain that were obtained from different regions of 4 subjects and from a whole mouse brain, was fractionated by sucrose gradient centrifugation, and 4 fractions floating at increasing densities of sucrose were collected (MB, main band; Di, dispersion; HB, heavy band; Pe pellet). For each sample, an equal amount of total protein (5 μg) was analyzed by immunoblotting for 3 major myelin proteins (MOG, MBP, PLP), 2 neuronal proteins (Caspr-2, PSD-95), and 1 astrocytic protein (GFAP). Blots are from different experiments and are intended only to show the relative distribution of each protein in the 4 fractions. Note that all samples of human myelin fractionated in a similar manner as rodent myelin, with enrichment of myelin proteins in the main band fraction and relatively minimal contamination of this fraction by neuronal and astrocytic proteins. *Samples used for MS analysis.

evaluate the relative contamination by neuronal and astrocytic proteins of the main band fractions, we analyzed 3 major myelin proteins (MOG, MBP, and PLP), 2 neuronal proteins [contactin-associated protein-2 (Caspr-2) and postsynaptic density-95 (PSD95)], and 1 astrocytic protein (GFAP) by immunoblotting (Fig. 1*B*). Our results indicate that all samples of human myelin fractionated in a similar manner as rodent myelin, with enrichment of myelin proteins in the main band fraction and relatively minimal contamination of this fraction by neuronal and astrocytic proteins.

Therefore, we conclude that sections of human brain do not need to be precisely matched for white matter content, patient age, or sex for representative proteomic analysis of human myelin and that the main band fractions from any of the myelin samples are suitable for representative MS analysis of human myelin proteins.

Protein Identification by Sequential 1-Dimensional PAGE and Liquid Chromatography/Tandem MS. Myelin samples from human subjects 3 and 4 (Fig. S1) and P35 mouse brains were separated by 1-dimensional gel electrophoresis, followed by peptide extraction and analysis by liquid chromatography and tandem MS (LC-MS/MS). This method avoids some of the limitations that are inherent to the commonly used 2D-PAGE separation method. For example, in 2D-PAGE, a protein must be prevalent enough to be excised. Using the 1-dimensional method, in-gel tryptic digestion of slices from the whole gel avoids the need for individual proteins to be recognized. One-dimensional PAGE also avoids the bias of 2D-PAGE that causes exclusion of specific protein populations (e.g., high-molecular-weight and basic proteins), which often remain unidentified; for example, MAG and MOG, which were not detected in previous studies (4, 6), were detected by the present technique.

Duplicate analysis was performed on all samples because earlier studies indicated that 1 MS analysis is not sufficient for exhaustive protein coverage (10). Consistently, in the present study, we detected additional proteins upon reanalysis of the same sample (average of 26% more proteins for human subjects 3 and 4 and 21% for mouse). However, despite this increase, certain known myelin proteins, such as connexin-32, remained unidentified.

Combining identified proteins from the duplicate analysis of both human subjects, we detected a total of 678 proteins in human myelin fractions (Fig. 2*A*). Similarly, 515 proteins were identified from mouse myelin fractions. Venn diagram comparisons showed that 308 proteins overlapped between human and mouse myelin. These proteins, belonging to various functional groups (Fig. 2*B*), are listed in Fig. 3 and will be the main focus of the present study. The complete list of all of the identified proteins is provided in Table S1.

Although some of the proteins that fell outside the commonly identified protein category may represent true biological differences between the species, for the most part it seems unlikely to be the case because of the technical limitations of MS. For example, proteins with slightly different amino acid sequences (e.g., human and mouse homologues) may have peptides with different physicochemical characteristics, resulting in the detection of these proteins in one species but not in the other. In addition, incomplete sampling of complex mixtures may preclude the identification of all proteins in a given sample (as described earlier). Consistent with this, immunoblot analysis of
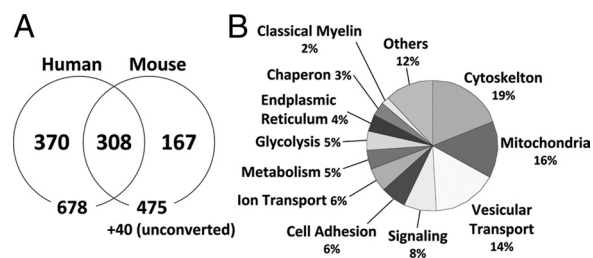
Fig. 2. Myelin proteins identified by 1-dimensional GelC-MS/MS. (*A*) Venn diagram shows the numbers of proteins identified by 1-dimensional GeLC-MS/MS shotgun approach in myelin fractions purified from human and mouse brains. A total of 678 proteins were identified from human and 515 from mouse. To allow for comparison, the mouse identifications were converted to the corresponding human UniProtKB database entry. Although 475 proteins converted successfully, 40 remained unconverted. The 308 proteins that overlapped are listed in Fig. 3, and the total proteins that were identified in the study are listed in supplementary Table S1. (*B*) Classification of 308 commonly identified proteins was done according to their function using SwissProt or via a literature search.

Fig. 2A: Human 370 | 308 | Mouse 167; 678 / 475 +40 (unconverted)

Fig. 2B: Classical Myelin 2%, Others 12%, Chaperon 3%, Cytoskelton 19%, Endplasmic Reticulum 4%, Mitochondria 16%, Glycolysis 5%, Vesicular Transport 14%, Metabolism 5%, Ion Transport 6%, Signaling 8%, Cell Adhesion 6%

Protein Name (Protein ID*, Gene Symbol**)		mRNA
Classical Myelin		
1 2',3'-cyclic-nucleotide 3'-phosphodiesterase (CN37, CNP)		0.8
2 Myelin-associated glycoprotein (MAG)		7.4
3 Myelin-oligodendrocyte glycoprotein (MOG)		3.8
4 Myelin basic protein (MBP)		5.3
5 Oligodendrocyte-specific protein (CLD11, CLDN11)		1.6
6 Myelin proteolipid protein (MYPR, PLP1)		5.1
Cytoskeleton		
1 Actin-binding protein anillin (ANLN)		>7.5
2 Adenylyl cyclase-associated protein 1 (CAP1)		1.2
3 α-internexin (AINX, INA)		0.3
4 Band 4.1-like protein 1 (E41L1, EPB41L1)		0.7
5 Band 4.1-like protein 2 (E41L2, EPB41L2)[Band 4.1 G]	IB	2.1
6 Band 4.1-like protein 3 (E41L3, EPB41L3)		1.4
7 β-centractin (ACTY, ACTR1B)		0.8
8 Catenin beta-1 (CTNB1, CTNNB1)		0.9
9 Cdc42 effector protein 1 (BORG5, CDC42SE1)		1.5
10 Cofilin-1 (COF1, CFL1)		0.9
11 Cytoplasmic dynein heavy chain 1 (DYHC, DYNC1H1)		x
12 Cytoplasmic FMR1-interacting protein 1 (CYFP1, FMR1)		1.0
13 Disheveled-associated activator of morphogenesis 2 (DAAM2)		3.3
14 Dynactin subunit 1 (DCTN1)		1.1
15 Dynactin subunit 2 (DCTN2)		1.2
16 Dynamin-1 (DYN1, DNM1)		0.3
17 Dynamin-2 (DYN2, DNM2)		2.1
18 Engulfment and cell motility protein 1 (ELMO1)		1.0
19 Ermin (Q8TAM6, KIAA1189)		x
20 Ezrin (EZRI, EZR)		1.0
21 Gelsolin (GELS, GSN)		3.2
22 Glial fibrillary acidic protein (GFAP)		2.8
23 Kinesin heavy chain isoform 5C (KIF5C)		1.2
24 Lethal(2,) giant larvae protein homolog 1 (L2GL1, LLGL1)		1.0
25 Microtubule-associated protein 1A (MAP1A)		0.5
26 Microtubule-associated protein 1B (MAP1B)		1.1
27 Microtubule-associated protein 2 (MAP2)		0.6
28 Microtubule-associated protein tau (TAU, MAPT)		0.9
29 Moesin (MOES, MSN)		1.4
30 Myosin-14 (MYH14)		0.8
31 Myosin-9 (MYH9)		0.9
32 Myosin-Id (MYO1D)		x
33 Myosin-Va (MYO5A)		x
34 Myosin-XVIIIa (MY18A, MYO18A)		x
35 NAD-dependent deacetylase sirtuin-2 (SIRT2)	IB	1.7
36 Neurofilament triplet H (NFH, NEFH)		0.3
37 Neurofilament triplet L (NFL, NEFL)		0.3
38 Neurofilament triplet M (NFM, NEFM)		0.4
39 p130Cas-associated protein (SNIP)		x
40 Plectin-1 (PLEC1)		1.3
41 Radixin (RADI, RDX)		x
42 Ras-related C3 botulinum toxin substrate 1 (RAC1)		1.5
43 Rho GDP-dissociation inhibitor 1 (GDIR, ARHGDIA)		0.9
44 Septin-11 (SEP11, SEPT11)		x
45 Septin-2 (SEPT2, SEPT2)	IB	1.8
46 Septin-4 (SEPT4, SEPT4)	IB	3.6
47 Septin-5 (SEPT5, SEPT5)		0.4
48 Septin-6 (SEPT6, SEPT6)		0.5
49 Septin-7 (SEPT7, SEPT7)	IB	1.9
50 Septin-8 (SEPT8, SEPT8)		3.2
51 Septin-9 (SEPT9, SEPT9)		0.7
52 Spectrin α chain (SPTA2, SPTAN1)		0.5
53 Spectrin β chain (SPTB2, SPTBN1)		1.0
54 Spectrin β chain (SPTN2, SPTBN2)		x
55 Tubulin β-4 chain (TBB4, TUBB4)		0.8
56 Tubulin β-6 chain (TBB6, TUBB6)		x
57 Tubulin polymerization-promoting protein (TPPP)		2.7
58 TPPP family member 3 (TPPP3)		5.8
Metabolism		
1 Acid ceramidase (ASAH1)		1.1
2 Aspartate aminotransferase (AATC, GOT1)		0.6
3 ATP-citrate synthase (ACLY)		0.8
4 Carbonic anhydrase 14 (CAH14, CA14)		1.1
5 Carbonic anhydrase 2 (CAH2, CA2)		2.3
6 Creatine kinase B-type (KCRB, CKB)		0.8
7 D-3-phosphoglycerate dehydrogenase (SERA, PHGDH)		1.5
8 Dihydropteridine reductase (DHPR, QDPR)	IB	2.6
9 Dimethylargininase-2 (DDAH2)		1.7
10 Dipeptidyl aminopeptidase-like protein 6 (DPP6)		0.6
11 Fatty acid synthase (FAS, FASN)		x
12 Glutamine synthetase (GLNA, GLUL)		0.9
13 Malate dehydrogenase (MDHC, MDH1)		0.4
14 Phosphoserine aminotransferase (SERC, PSAT1)		1.6
15 Transketolase (TKT)		1.4
Glycolysis		
1 α-enolase (ENOA, ENO1)		0.8
2 Fructose-bisphosphate aldolase A (ALDOA)		0.8
3 Fructose-bisphosphate aldolase C (ALDOC)		0.6
4 γ-enolase (ENOG, ENO2)		0.5
5 Glucose-6-phosphate isomerase (G6PI, GPI)		0.7
6 Glyceraldehyde-3-phosphate dehydrogenase (G3P, GAPDH)		0.7
7 Hexokinase-1 (HXK1, HK1)		0.4
8 L-lactate dehydrogenase B chain (LDHB)		0.8
9 Phosphofructo-1-kinase isozyme A (K6PF, PFKM)		x
10 Phosphofructokinase 1 (K6PP, PFKP)		0.6
11 Phosphoglycerate kinase 1 (PGK1)		0.7
12 Phosphoglycerate mutase 1 (PGAM1)		0.8
13 Pyruvate kinase isozymes M1/M2 (KPYM, PKM2)		0.7
14 Triosephosphate isomerase (TPIS, TPI1)		0.4
Endoplasmic Reticulum		
1 40S ribosomal protein S3 (RS3, RPS3A)		1.3
2 78 kDa glucose-regulated protein (GRP78, HSPA5)		1.1
3 Elongation factor 1-α 2 (EF1A2, EEF1A2)		0.3
4 Estradiol 17-beta-dehydrogenase 12 (DHB12, HSD17B3)		1.6
5 Heme oxygenase 2 (HMOX2)		0.9
6 Membrane-assoc. progesterone receptor component 1 (PGRC1, PGRMC1)		2.3
7 Protein disulfide-isomerase A3 (PDIA3)		1.8
8 Reticulon-1 (RTN1,)		0.4
9 Reticulon-4 (RTN4)		1.0
10 Retinol dehydrogenase 11 (RDH11)		1.1
11 Ribophorin I (RIB1, RPN1)		1.2
12 Sarcoplasmic/ER Ca2+ ATPase 2 (AT2A2, ATP2A2)		x
13 Transitional ER ATPase (TERA, VCP)		0.9

Protein Name (Protein ID*, Gene Symbol**)		mRNA
Vesicular Transport		
1 ADP-ribosylation factor 4 (ARF4)		1.0
2 α-soluble NSF attachment protein (SNAA, NAPA)		0.7
3 Amphiphysin (AMPH)		0.3
4 AP-1 complex subunit β-1 (AP1B1)		1.3
5 AP-2 complex subunit α-1 (AP2A1)		x
6 AP-2 complex subunit α-2 (AP2A2)		0.7
7 B-cell receptor-associated protein 31 (BAP31, BCAP31)		0.9
8 Charged multivesicular body protein 4b (CHM4B, CHMP4B)		x
9 Chloride intracellular channel protein 4 (CLIC4)	IB	2.8
10 Clathrin coat assembly protein AP180 (AP180, SNAP91)		x
11 Clathrin heavy chain 1 (CLH1, CLTC)		0.7
12 Differentiation-related gene 1 protein (NDRG1)	IB	2.9
13 Dihydropyrimidinase-related protein 1 (DPYL1, DPYSL1)		0.5
14 Dihydropyrimidinase-related protein 2 (DPYL2, DPYSL2)		1.5
15 Dihydropyrimidinase-related protein 3 (DPYL3, DPYSL3)		1.5
16 γ-soluble NSF attachment protein (SNAG, NAPG)		x
17 PACSIN1 (PACN1, PACSIN1)		x
18 Probable phospholipid-transporting ATPase IA (AT8A1, ATP8A1)		x
19 Rab GDP dissociation inhibitor alpha (GDIA, ARHGDIA)		0.9
20 Rab GDP dissociation inhibitor beta (GDIB, ARHGDIB)		x
21 Ras-related protein Rab-14 (RAB14)		1.2
22 Ras-related protein Rab-1B (RAB1B)		0.9
23 Ras-related protein Rab-3A (RAB3A)		0.3
24 Ras-related protein Rab-5A (RAB5A)		1.1
25 Ras-related protein Rab-5C (RAB5C)		0.8
26 Ras-related protein Rab-6A (RAB6A)		0.9
27 Ras-related protein Ral-A (RALA)		>7.5
28 Ras-related protein Ral-B (RALB)		0.8
29 Reticulon-3 (RTN3)		0.9
30 Synapsin-1 (SYN1)		0.3
31 Synaptic vesicle glycoprotein 2A (SV2A)		0.3
32 Synaptic vesicle membrane protein VAT-1 homolog (VAT1)		1.4
33 Synaptotagmin-1 (SYT1)		0.4
34 Syntaxin-12 (STX12)		1.4
35 Syntaxin-1A (STX1A)		0.6
36 Syntaxin-1B (STX1B)		x
37 Syntaxin-4 (STX4)		1.4
38 Syntaxin-6 (STX6)		1.0
39 Syntaxin-7 (STX7)		1.2
40 Syntaxin-binding protein 5 (STXB5, STXBP5L)		0.6
41 V-ATPase 116 kDa isoform a1 (VPP1, ATP6V0A1)		x
42 VAMP-associated protein A (VAPA)		1.1
43 VAMP-associated protein B/C (VAPB)		0.8
44 Vesicle-fusing ATPase (NSF)		0.3
Ion Transport		
1 Basolateral Na-K-Cl symporter (S12A2, SLC12A2)		1.1
2 Excitatory amino acid transporter 1 (EAA1, SLC1A3)		0.6
3 Excitatory amino acid transporter 2 (EAA2, SLC1A2)		0.4
4 FXYD domain-containing ion transport regulator 6 (FXYD6)		0.7
5 Plasma membrane Ca2+-transporting ATPase 1 (AT2B1, ATP2B1)		0.6
6 Plasma membrane Ca2+-transporting ATPase 2 (AT2B2, ATP2B2)		x
7 K+ voltage-gated channel subfamily A member 1 (KCNA1)		1.5
8 Na+/Ca2+ exchanger 2 (NAC2, SLC8A2)		0.4
9 Na+/K+ transporting ATPase subunit α-1 (AT1A1, ATP1A1)		0.5
10 Na+/K+ transporting ATPase subunit α-3 (AT1A3, ATP1A3)		0.3
11 Na+/K+ transporting ATPase subunit β-1 (AT1B1, ATP1B1)		x
12 Vacuolar ATP synthase catalytic subunit A (VATA, ATP6V1A)		x
13 Vacuolar ATP synthase subunit B (VATB2, ATP6V1B2)		x
14 Vacuolar ATP synthase subunit C 1 (VATC1, ATP6V1C1)		x
15 Vacuolar ATP synthase subunit D (VATD, ATP6V1D)		0.7
16 Vacuolar ATP synthase subunit E 1 (VATE1, ATP6V1E1)		x
17 Vacuolar ATP synthase subunit H (VATH, ATP6V1H)		x
18 Voltage-gated K+ channel subunit β-2 (KCAB2, KCNAB2)		x
Cell Adhesion		
1 ADAM 22 (ADA22, ADAM22)		1.0
2 Cadherin-13 (CAD13, CDH13)		x
3 CD166 antigen (CD166, ALCAM)		x
4 CD81 antigen (CD81)		1.3
5 Cell adhesion molecule 4 (CADM4)		x
6 Contactin-1 (CNTN1)		>7.5
7 Contactin-2 (CNTN2)		>7.5
8 Contactin-associated protein 1 (CNTP1, CNTNAP1)		1.5
9 Flotillin-2 (FLOT2)		1.2
10 Immunoglobulin superfamily member 8 (IGSF8)		x
11 Junctional adhesion molecule C (JAM3)		2.9
12 Limbic system-associated membrane protein (LSAMP)		x
13 Neural cell adhesion molecule 1 (NCA11, NCAM1)		1.1
14 Neural cell adhesion molecule 2 (NCAM2)		1.1
15 Neurofascin (NFASC)		0.9
16 Neuronal growth regulator 1 (NEGR1)		x
17 Neurotrimin (NTRI, HNT)		x
18 Tenascin-R (TENR, TNR)		1.1
19 Thy-1 membrane glycoprotein (THY1)		0.6
20 Tight junction protein ZO-2 (ZO2, TJP2)		3.4
Signaling		
1 14-3-3 protein β/α (1433B, YWHAB)		0.4
2 14-3-3 protein θ (1433T, YWHAQ)		2.2
3 14-3-3 protein ζ/δ (1433Z, YWHAZ)		0.6
4 CaMK-II subunit α (KCC2A, CAMK2A)		0.8
5 CaMK-II subunit β (KCC2B, CAMK2B)		1.1
6 cAMP-dependent protein kinase I-α regulatory subunit (KAP0, PRKAR1A)		1.0
7 GTPase Hras (RASH, HRAS)		1.0
8 GTPase KRas (RASK, KRAS)		0.6
9 Guanine nucleotide-binding protein α-13 subunit (GNA13)		x
10 Guanine nucleotide-binding protein G(i) α-2 subunit (GNAI2)		1.4
11 Guanine nucleotide-binding protein G(k) subunit α (GNAI3)		1.3
12 Guanine nucleotide-binding protein G(o) subunit α 1 (GNAO1)		0.6
13 Guanine nucleotide-binding protein G(z) subunit α (GNAZ)		1.2
14 Guanine nucleotide-binding protein subunit α-11 (GNA11)		0.8
15 MAGUK p55 subfamily member 2 (MPP2)		1.0
16 MAPK/ERK kinase 1 (MP2K1, MAP2K1)		0.6
17 Phosphatidylinositol-5-phosphate 4-kinase type-2 α (PI42A, PIP4K2A)		3.5
18 Phosphoinositide phospholipase C (PLCB1)		0.3
19 Protein kinase C gamma type (KPCG, PRKAG2)		0.9
20 Ras-related protein Rap-2a (RAP2A)		0.7
21 Receptor expression-enhancing protein 5 (REEP5)		0.7
22 Serine/threonine-protein phosphatase 2A (2AAA, PPP2R5B)		0.8
23 Serine/threonine-protein phosphatase 2B (PP2BA, PPP3CA)		0.3
24 Signal regulatory protein α-1 (SHPS1, SIRPA)		x

(mRNA sub-columns: W/G, O, N, A, U)

Fig. 3. (*Figure continues on the opposite page.*)

Mitochondria	mRNA
1 Succinyl-CoA synthetase subunit α (SUCA, SUCLG1)	x
2 60 kDa heat shock protein (CH60, HSPD1)	x
3 Acetyl-CoA acetyltransferase (THIL, ACAT1)	1.4
4 Aconitate hydratase (ACON, ACO2)	0.9
5 ADP/ATP translocase 1 (ADT1, SLC25A4)	0.7
6 ADP/ATP translocase 2 (ADT2, SLC25A5)	0.8
7 Aspartate aminotransferase (AATM, GOT2)	0.8
8 ATP synthase B chain (AT5F1, ATP5A1)	0.6
9 ATP synthase D chain (ATP5H)	0.9
10 ATP synthase e chain (ATP5I)	1.6
11 ATP synthase gamma chain (ATPG, ATP5C1)	1.0
12 ATP synthase subunit α (ATPA, ATP5A1)	1.6
13 ATP synthase subunit β (ATPB, ATP5B)	0.7
14 ATP synthase subunit O (ATPO, ATP5O)	0.8
15 Ca2+ binding mitochondrial carrier protein Aralar1 (CMC1, SLC25A12)	0.5
16 Creatine kinase (KCRU, CKB)	0.8
17 Cytochrome c (CYC, CYCS)	0.7
18 Cytochrome c oxidase subunit 2 (COX2,)	0.7
19 Cytochrome c oxidase subunit 4 isoform 1 (COX41, COX4I1)	0.9
20 Cytochrome c oxidase subunit 5A (COX5A)	0.8
21 Cytochrome c1 heme protein (CY1, CYC1)	0.9
22 Dihydrolipoyl dehydrogenase (DLDH, DLD)	x
23 Dynamin-like 120 kDa protein (OPA1)	0.8
24 Enoyl-CoA hydratase (ECHM, ECH1)	0.9
25 Glutamate dehydrogenase 1 (DHE3, GLUD1)	0.7
26 Isocitrate dehydrogenase [NAD] subunit α (IDH3A)	0.8
27 Isocitrate dehydrogenase [NAD] subunit β (IDH3B)	1.0
28 Malate dehydrogenase (MDHM, MDH1)	0.4
29 Mitochondrial 2-oxoglutarate/malate carrier protein (M2OM, SLC25A11)	1.0
30 Mitochondrial inner membrane protein (IMMT)	0.7
31 NADH dehydrogenase [ubiquinone] flavoprotein 2 (NDUV2, NDUFV2)	0.9
32 NADH dehydrogenase [ubiquinone] iron-sulfur protein 3 (NDUS3, NDUFS3)	x
33 NADH-cytochrome b5 reductase 3 (NB5R3, CYB5R3)	x
34 NADH-ubiquinone oxidoreductase 39 kDa subunit (NDUA9, NDUFA9)	0.9
35 NADH-ubiquinone oxidoreductase 75 kDa subunit (NDUS1, NDUFS1)	1.1
36 Phosphate carrier protein (MPCP, SLC25A3)	1.0
37 Prohibitin (PHB)	1.1
38 Prohibitin-2 (PHB2)	1.0
39 Pyruvate dehydrogenase complex E2 subunit (ODP2, DLAT)	x
40 Pyruvate dehydrogenase E1 component subunit β (ODPB, PDHB)	1.3
41 Sideroflexin-3 (SFXN3)	1.0
42 Succinate dehydrogenase [ubiquinone] iron-sulfur subunit (DHSB, SDHB)	0.9
43 Succinyl-CoA:3-ketoacid-coenzyme A transferase 1 (SCOT, OXCT1)	0.7
44 Ubiquinol-cytochrome c reductase iron-sulfur subunit (UCRI, UQCRFS1)	0.8
45 Cytochrome b-c1 complex subunit 1 (UQCR1, UQCRC1)	0.7
46 Cytochrome b-c1 complex subunit 2 (UQCR2, UQCRC2)	0.6
47 Voltage-dependent anion-selective channel protein 1 (VDAC1)	0.6
48 Voltage-dependent anion-selective channel protein 2 (VDAC2)	0.9
49 Voltage-dependent anion-selective channel protein 3 (VDAC3)	0.6

Chaperone	mRNA
1 Calnexin (CALX, CANX)	1.0
2 Heat shock 70 kDa protein 12A (HS12A, HSPA12A)	x
3 Heat shock cognate 71 kDa protein (HSP7C, HSPA8)	0.8
4 Heat shock protein 90 kDa β member 1 (ENPL, HSP90B1)	x
5 Heat shock protein HSP 90-α (HS90A, HSP90AA1)	1.0
6 Heat shock protein HSP 90-β (HS90B, HSP90AB1)	0.9
7 Heat shock-related 70 kDa protein 2 (HSP72, HSPA2)	x
8 T-complex protein 1 subunit α (TCPA, TCP1)	x
9 T-complex protein 1 subunit β (TCPB, CCT2)	0.8
10 T-complex protein 1 subunit δ (TCPD, CCT4)	1.0

Others	mRNA
1 26S protease regulatory subunit 8 (PRS8, PSMD8)	0.9
2 4F2 cell-surface antigen heavy chain (4F2, SLC3A2)	1.0
3 Annexin A5 (ANXA5)	1.6
4 Brain acid soluble protein 1 (BASP, BASP1)	0.3
5 Breast carcinoma amplified sequence 1 (BCAS1)	3.3
6 Choline transporter-like protein 1 (CTL1, SLC44A1)	x
7 EH domain-containing protein 3 (EHD3,)	0.4
8 Endonuclease domain-containing 1 protein (ENDD1, ENDOD1)	x
9 Flotillin-1 (FLOT1)	1.1
10 Glutathione S-transferase Mu 1 (GSTM1)	0.8
11 Glutathione S-transferase P (GSTP1)	1.1
12 Growth-arrest-specific protein 7 (GAS7)	1.2
13 Hemoglobin subunit α (HBA, HBA1)	1.1
14 Histone deacetylase 11 (HDA11, HDAC11)	x
15 Leucine-rich repeat LGI family member 3 (LGI3,)	x
16 Leucine-rich repeat-containing protein 57 (LRC57, LRRC57)	x
17 Myc box-dependent-interacting protein 1 (BIN1)	2.8
18 Neuronal membrane glycoprotein M6-a (GPM6A)	0.4
19 Nucleoside diphosphate kinase A (NDKA, NME1)	x
20 Nucleoside diphosphate kinase B (NDKB, NME2)	x
21 Otubain-1 (OTUB1)	0.7
22 Pancreas/duodenum homeobox protein 1 (PDX1)	x
23 Paralemmin (PALM)	0.5
24 Peroxiredoxin-2 (PRDX2)	0.7
25 Protein C14orf166 (CN166, C14orf166)	1.5
26 Protein FAM49A (FA49A, FAM49A)	x
27 Protein FAM49B (FA49B, FAM49B)	x
28 Protein FAM62A (FA62A, FAM62A)	x
29 Protein NipSnap1 (NIPS1, NIPSNAP1)	0.5
30 Protein S100-B (S100B)	4.3
31 Protein-arginine deiminase type-2 (PADI2)	3.5
32 Serum albumin (ALBU, TTR)	1.4
33 Similar to metallo-β-lactamase superfamily protein (Q8IY16, LOC153364)	x
34 Tetratricopeptide repeat protein 35 (TTC35)	1.8
35 Transcriptional activator protein Pur-α (PURA)	1.4
36 Ubiquitin carboxyl-terminal hydrolase isozyme L1 (UCHL1)	0.5
37 Uncharacterized protein C1orf198 (CA198, C1orf198)	x

Fig. 3. Proteins of human myelin and microarray analysis of human white and gray matter: Functional categorization of identified proteins and comparison with other myelin proteomes and transcriptomes of OL-, astrocyte-, or neuron-enriched genes. The 308 proteins commonly identified by MS in human and mouse myelin fractions are categorized into several functional subgroups. Relative intensities of mRNA signals for these proteins was determined by microarray analyses of human white (W) and gray matter (G). Many of these transcripts are expressed at higher levels in OL-rich white over gray matter, shown as fold enrichment (i.e., W/G ratio). In addition, to help ascertain the cellular origins of the proteins identified in our proteome, the relative enrichment of their transcripts in purified OLs (red squares in column O), neurons (column N), or astrocytes (column A) was determined through analysis of the transcriptome database of Cahoy et al. (8) and other studies (12–18) of OLs (tan squares in column O). Comparison of the identified proteins in this study with other myelin proteomes (4–7) has confirmed more than 50% of the identified proteins and revealed the presence of 163 additional proteins in myelin that have not previously been reported in any other proteome (column U). *Human protein ID in the UniProt Knowledgebase; see Table S1 for corresponding mouse IDs. **Gene symbols as described in National Center for Biotechnology Information database are given only when different from protein ID. *mRNA*, microarray analysis; *X*, not present in array chip or transcripts below reliable detection threshold; *IB*, proteins validated by immunoblotting in Fig. 4.

6 proteins, as an example, showed that proteins that were not identified by MS in one species could be identified by immunoblot analysis in that species (Fig. S3). MS identifications also may vary from protein to protein, even within the same family. For example, among the tetraspanin family, CD9 and plasmolipin were identified only in human, even though they also were expressed in mouse myelin, as shown by immunoblotting for CD9 (Fig. S3) and by a literature search for plasmolipin (11). CD81, to the contrary, was identified in both species, whereas MAL/MVP17 was not detected in either human or mouse samples because its amino acid sequence precludes it from MS detection (see SI Methods). These data emphasize the limitations of MS analysis and show that non-identification of a protein by MS does not prove conclusively that it is absent from the sample. Thus, the current overlap that is seen between human and rodent proteomes is most likely an underestimation.

Comparison of the commonly identified proteins in this study with 4 other myelin proteomes (4–7) has validated more than 50% of these proteins. Considering the technical differences among the 5 approaches, the significant overlap provides considerable confidence in their identification. This comparison also has revealed the presence of 163 proteins that have not previously been described in any other proteome, thus providing insights into the complex composition of myelin (Fig. 3 and Fig. S2).

Validation of MS Identification. The rigorously purified main band myelin fraction that was used in this study was highly enriched

in myelin proteins, and negligible amounts of neuronal and astrocytic proteins were detected on the immunoblots (Fig. 1B). However, it is difficult, if not impossible, to obtain totally "pure myelin," presumably because of high-affinity interactions between myelin and axolemmal membranes (9). Given the high sensitivity of MS detection, it is likely that some axonal or astrocytic proteins exist in our (and previous) myelin proteomes. To address this issue and increase confidence in the MS identification of proteins in purified myelin fractions, we argued that if a protein or mRNA that encodes a protein is expressed by OLs, the cellular source of myelin, it should be a true myelin component. We therefore used different criteria to help ascertain the cellular origins of proteins that were identified in our proteome.

First, we compared our database with other studies, primarily the transcriptome database of OLs, neurons, and astrocytes that were isolated from rodent brains (8, 12–18). Among the 308 proteins, there were at least 111 proteins in our myelin proteome whose mRNA or protein was expressed by OLs (Fig. 3, column O, red and tan boxes). Interestingly, 64 of these also were highly enriched in OLs, not in neurons, and rarely in astrocytes [supplemental tables 4–6 and 17–19 of Cahoy et al (8); see SI Methods]. This group of proteins, which are short-listed in Fig. S2, is likely to play a preferential role in OL/myelin biology. Some mRNAs, which were expressed in 2 or more cell types, possibly have common functions in these cell types. For example, mRNA that encodes RAC1 is expressed by OLs and astrocytes.
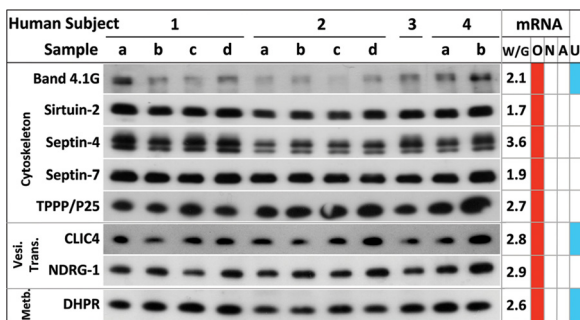
Human Subject	1				2				3	4		mRNA				
Sample	a	b	c	d	a	b	c	d		a	b	W/G	O	N	A	U
Cytoskeleton Band 4.1G												2.1				
Sirtuin-2												1.7				
Septin-4												3.6				
Septin-7												1.9				
TPPP/P25												2.7				
Vesi. Trans. CLIC4												2.8				
NDRG-1												2.9				
Metb. DHPR												2.6				

Fig. 4. Immunoblot analysis of select proteins from different subgroups identified by MS to validate their presence in human myelins. Eight proteins, belonging to different functional subgroups, were selected as an example to validate their identification by MS in human myelin fractions. The criteria for selection was that (*i*) their mRNA was enriched in OLs (column O) but not in neurons (column N) or astrocytes (column A), and (*ii*) their mRNA expression was at least 1.7 fold higher in human white matter than gray matter. All 8 proteins were detected reproducibly by immunoblotting in each of the 11 human myelin samples from 4 subjects, providing increased confidence in their MS detection. Three of them have not been identified in previous rodent myelin proteomes (column U). *TPPP/P25*, tubulin polymerization-promoting protein; *CLIC4*, chloride intracellular channel protein 4; *DHPR*, dihydropteridine reductase; *NDRG1*, N-myc downstream-regulated gene 1; *Vesic. Trans*, vesicular transport; *Metb*, metabolism.

RAC1 signaling is important for myelin sheath formation (19) and growth of astrocytic processes (20).

Second, we quantified mRNAs that encoded the 308 proteins in human CNS white and gray matter by microarray analysis. Transcripts of several proteins were highly expressed in the OL-rich white matter compared with gray matter, suggesting an association of these transcripts with myelin-producing OLs in vivo. Conversely, some other proteins, such as neurofilament peptides, which were found at low levels in human white compared with gray matter, were obviously axonal proteins that co-purified with myelin fractions. White-to-gray matter (W/G) ratios are shown in Fig. 3 to facilitate such comparisons for all the proteins. In addition, when the W/G ratios of the short-listed proteins were examined (Fig. S2), we found that approximately half the transcripts that were enriched in OLs also were elevated 1.5 to 7.5 fold in human white over gray matter. Combining the 2 criteria has further narrowed the selection of candidates that are true myelin proteins, many of which have not been reported previously (Fig. S2).

Third, we searched for the tissue localization of mRNAs of select proteins in mouse brain from the Allen Brain Atlas (http://www.brain-map.org). The in situ hybridization results showed that expression of several transcripts that encoded these proteins was detected in the white matter tracts of adult mouse brain.

Last, to verify the MS and microarray identification, as an example, we performed immunoblot analysis (Fig. 4) on 8 proteins that were selected among 64 proteins from the short list (Fig. S2) and belonged to different functional subgroups whose mRNAs were expressed at high levels in human white matter over gray matter and whose mRNA was enriched in purified rodent OLs but not neurons or astrocytes. We reliably detected the presence of all 8 proteins [band 4.1 G, sirtuin-2, septin-4, septin-7, tubulin polymerization-promoting protein, chloride intracellular channel protein 4 (CLIC4), dihydropteridine reductase (DHPR), and N-myc downstream-regulated gene 1 (NDRG1)] on immunoblots of 11 different human myelin preparations from 4 human subjects. In addition, we also verified 6 other identified proteins (Rac-1, CD81, contactin-1, reticulon-4, RalA, and creatine kinase B) by immunoblotting.

Together, this analysis provides increased confidence in our MS detection of numerous proteins that are present in purified human myelin.

Functional Implications of Proteins Identified in Myelin Proteome. As expected, several classical myelin proteins, such as CNP, MAG, MBP, MOG, OSP, and PLP, were found in both human and mouse myelin, and are known to constitute more than 90% of total myelin proteins in the rodent. It is becoming clear from numerous proteomic analyses (4–7) that there are in fact myriad additional proteins that are present in rodent myelin. The highest number that has been identified in a single study is approximately 160 (7), but the number has been increased to 515 in the present analysis. These quantitatively "minor" proteins of myelin may not necessarily be "functionally minor," as many of them play important roles in OL and myelin biology. For example, ermin, an OL protein involved in cytoskeletal rearrangement during the late wrapping and/or compaction of myelin (17), and Necl4, involved in myelination in the peripheral nervous system (21, 22), were identified in this study but not in previous studies, illustrating the usefulness of this sensitive proteomic approach for identifying functionally relevant minor myelin proteins.

Among the 308 proteins that were identified by this approach, we detected a variety of proteins that were involved in signaling, cytoskeletal organization, cell adhesion, protein trafficking and vesicular transport, ion transport, endoplasmic reticulum and mitochondrial function, and energy metabolism (Figs. 2*B* and 3 and Fig. S4). All these functions are critical for myelin biogenesis and maintenance.

The presence of a large number of cytoskeletal proteins in the myelin proteome was not unexpected, because the cytoskeleton is a necessary component for formation and maintenance of the myelin sheath (23), including targeting of the major myelin proteins and mRNA to the myelin membrane (24, 25). In addition to septin-4 and septin-7, which were verified by immunoblot analysis, several other members of the septin family (septins 2, 5, 6, 8, 9, and 11) were also detected in the myelin proteome. Microtubule proteins that were identified included β4-tubulin, selectively expressed by OLs (16); microtubule-associated protein (MAP) 1B, expressed by OLs in vitro (12); and MAP1A, MAP2, and Tau. Interestingly, Band 4.1G and tubulin polymerization-promoting protein, reported in OLs (26), have been identified and verified by immunoblot to be present in myelin.

Biogenesis and maintenance of myelin require vesicular transport for the sorting and trafficking of proteins and lipids by OLs to the myelin membrane. Several transport proteins from related families were identified in our study from both human and rodent. For example, the small GTPase family of proteins, including those that are expressed in OLs (Rab3a, 5a, 5c, 6, and RalA) (13, 27); syntaxins, involved in vesicle fusion, including syntaxin-4, which is up-regulated during OL differentiation (15); and clathrin coat-related proteins, involved in vesicle budding, including clathrin heavy chain, AP1b1, APa1, and AP2a2, were identified. The multifunctional protein CLIC4, which exists in both soluble and membrane forms and is known to be localized to several membrane systems, including the trans-Golgi network, secretory vesicles, and plasma membrane (28), was detected for the first time in myelin membrane by both MS and immunoblotting (Figs. 3 and 4). NDRG1, a cytoplasmic protein that is expressed by OLs (29) and validated by immunoblotting in human myelin (Fig. 4), has been identified as a Rab4a effector recruited to recycling/sorting endosomes in cell lines (30).

Several mitochondrial proteins have been consistently identified in "purified" myelin fractions by proteomic analysis (4–7). The present study also found a large number of mitochondrial proteins in myelin of both human and mouse, including TCA cycle enzymes (e.g., aconitate hydratase) and respiratory chain enzymes (e.g., cytochrome c). Although the possibility remains

NEUROSCIENCE

that they represent a contamination of myelin (5, 7), mitochondria are known to localize in OL processes (31) and are present in peripheral nervous system (32) and CNS myelin (33). It is likely that myelin internode mitochondria provide the ATP that is needed for the expansion of myelin membranes during myelination. In addition, mitochondrial dysfunction occurs in various demyelinating neurological diseases, suggesting the importance to human diseases.

In this large-scale proteomic analysis of human and mouse myelin, with the use of multifocal approaches, we have presented evidence that promotes confidence in our MS identification. This study has vastly expanded the repertoire of myelin proteins and revealed a more complete picture of the composition of myelin proteins that have a variety of possible functions that are relevant for myelin biogenesis and maintenance. This database is expected to serve as a roadmap for future in-depth study of both human and mouse myelin biology and the understanding of human diseases that pertain to myelin pathology.

Materials and Methods

Myelin Purification. Postmortem brains from 4 human subjects with no neurological disorders were dissected as described previously (34) and summarized in Fig. S1. Eleven sections with varying white matter content were cut from these brains. Myelin was purified from these samples and from mouse brain (postnatal day 35; C57BL/6) by sucrose density gradient centrifugation as described previously (9). Four fractions were collected, floating at different sucrose densities: main band (12.0%–22.5%), ''dispersion'' (22.5%–25.4%), ''heavy band'' (25.5%–26.9%), and ''pellet.'' Total protein concentrations were determined by BCA protein assay (Bio-Rad).

MS Analysis. MS was performed as described previously (35). Briefly, main band myelin fractions (150 μg protein) from human subjects 3 and 4 and mouse were separated by 1-dimensional gel electrophoresis, followed by colloidal Coomassie staining. Gel lanes were sliced, trypsinized, and extracted. Peptides were analyzed by LC-MS/MS using an LTQ ion-trap mass spectrometer. Proteins that were identified by the presence of at least 2 distinct peptides in the same sample were accepted as high-confidence identification. Duplicate analyses were performed for each sample. Further details of MS and data analysis are provided in SI Methods.

Immunoblotting. Total proteins from purified human and mouse myelin were separated by SDS/PAGE, transferred onto polyvinylidene difluoride membranes, incubated with primary antibody (1 h at room temperature) and horseradish peroxidase-conjugated secondary antibodies (1 h at room temperature), and diluted in blocking solution (5% nonfat dry milk in Tris-buffered saline solution with 0.2% Tween 20). Blots were visualized using enhanced chemiluminescence (GE Healthcare). Details of antibodies are given in SI Methods.

Microarray Analysis. Eight samples each of white matter or gray matter tissue from the same tissue block were collected from 3 postmortem human brains (Fig. S1). RNA was extracted, and microarray and data analysis were performed as described previously (34) (see SI Methods).

1. Trapp BD, Kidd GJ (2004) Structure of the myelinated axon. *Myelin Biology and Disorders*, ed Lazzarini RA (Elsevier, New York), pp 3–27.
2. Davis KL, et al. (2003) White matter changes in schizophrenia: evidence for myelin-related dysfunction. *Arch Gen Psychiatry* 60:443–456.
3. Peters A (2002) The effects of normal aging on myelin and nerve fibers: a review. *J Neurocytol* 31:581–593.
4. Taylor CM, et al. (2004) Proteomic mapping provides powerful insights into functional myelin biology. *Proc Natl Acad Sci USA* 101:4643–4648.
5. Roth AD, Ivanova A, Colman DR (2005) New observations on the compact myelin proteome. *Neuron Glia Biol* 2:15–21.
6. Vanrobaeys F, Van Coster R, Dhondt G, Devreese B, Van Beeumen J (2005) Profiling of myelin proteins by 2D-gel electrophoresis and multidimensional liquid chromatography coupled to MALDI TOF-TOF mass spectrometry. *J Proteome Res* 4:2283–2293.
7. Werner HB, et al. (2007) Proteolipid protein is required for transport of sirtuin 2 into CNS myelin. *J Neurosci* 27:7717–7730.
8. Cahoy JD, et al. (2008) A transcriptome database for astrocytes, neurons, and oligodendrocytes: a new resource for understanding brain development and function. *J Neurosci* 28:264–278.
9. Menon K, et al. (2003) The myelin-axolemmal complex: biochemical dissection and the role of galactosphingolipids. *J Neurochem* 87:995–1009.
10. Wu L, et al. (2007) Global survey of human T leukemic cells by integrating proteomics and transcriptomics profiling. *Mol Cell Proteomics* 6:1343–1353.
11. Cochary EF, Bizzozero OA, Sapirstein VS, Nolan CE, Fischer I (1990) Presence of the plasma membrane proteolipid (plasmolipin) in myelin. *J Neurochem* 55:602–610.
12. Fischer I, Konola J, Cochary E (1990) Microtubule associated protein (MAP1B) is present in cultured oligodendrocytes and co-localizes with tubulin. *J Neurosci Res* 27:112–124.
13. Huber LA, Madison DL, Simons K, Pfeiffer SE (1994) Myelin membrane biogenesis by oligodendrocytes. Developmental regulation of low molecular weight GTP-binding proteins. *FEBS Lett* 347:273–278.
14. Fink D, Knapp PE, Mata M (1996) Differential expression of Na,K-ATPase isoforms in oligodendrocytes and astrocytes. *Dev Neurosci* 18:319–326.
15. Madison DL, Krueger WH, Cheng D, Trapp BD, Pfeiffer SE (1999) SNARE complex proteins, including the cognate pair VAMP-2 and syntaxin-4, are expressed in cultured oligodendrocytes. *J Neurochem* 72:988–998.
16. Terada N, et al. (2005) Beta IV tubulin is selectively expressed by oligodendrocytes in the central nervous system. *Glia* 50:212–222.
17. Brockschnieder D, Sabanay H, Riethmacher D, Peles E (2006) Ermin, a myelinating oligodendrocyte-specific protein that regulates cell morphology. *J Neurosci* 26:757–762.
18. Dumont D, et al. (2007) Characterization of mature rat oligodendrocytes: a proteomic approach. *J Neurochem* 102:562–576.
19. Thurnherr T, et al. (2006) Cdc42 and Rac1 signaling are both required for and act synergistically in the correct formation of myelin sheaths in the CNS. *J Neurosci* 26:10110–10119.
20. Kalman D, Gomperts SN, Hardy S, Kitamura M, Bishop JM (1999) Ras family GTPases control growth of astrocyte processes. *Mol Biol Cell* 10:1665–1683.
21. Maurel P, et al. (2007) Nectin-like proteins mediate axon Schwann cell interactions along the internode and are essential for myelination. *J Cell Biol* 178:861–874.
22. Spiegel I, et al. (2007) A central role for Necl4 (SynCAM4) in Schwann cell-axon interaction and myelination. *Nat Neurosci* 10:861–869.
23. Trapp BD, Pfeiffer SE, Anitei M, Kidd GJ (2004) Cell biology of myelin assembly. *Myelin Biology and Disorders*, ed Lazzarini RA (Elsevier, New York), pp 29–55.
24. Benjamins JA, Nedelkoska L (1994) Maintenance of membrane sheets by cultured oligodendrocytes requires continuous microtubule turnover and Golgi transport. *Neurochem Res* 19:631–639.
25. Ainger K, et al. (1993) Transport and localization of exogenous myelin basic protein mRNA microinjected into oligodendrocytes. *J Cell Biol* 123:431–441.
26. Song YJ, et al. (2007) p25alpha relocalizes in oligodendroglia from myelin to cytoplasmic inclusions in multiple system atrophy. *Am J Pathol* 171:1291–1303.
27. Anitei M, Cowan AE, Pfeiffer SE, Bansal R (2009) Role for Rab3a in oligodendrocyte morphological differentiation. *J Neurosci* 87:342–352.
28. Ashley RH (2003) Challenging accepted ion channel biology: p64 and the CLIC family of putative intracellular anion channel proteins. *Mol Membr Biol* 20:1–11.
29. Berger P, Sirkowski EE, Scherer SS, Suter U (2004) Expression analysis of the N-Myc downstream-regulated gene 1 indicates that myelinating Schwann cells are the primary disease target in hereditary motor and sensory neuropathy-Lom. *Neurobiol Dis* 17:290–299.
30. Kachhap SK, et al. (2007) The N-Myc down regulated Gene1 (NDRG1) is a Rab4a effector involved in vesicular recycling of E-cadherin. *PLoS ONE* 2:e844.
31. Simpson PB, Mehotra S, Lange GD, Russell JT (1997) High density distribution of endoplasmic reticulum proteins and mitochondria at specialized Ca2+ release sites in oligodendrocyte processes. *J Biol Chem* 272:22654–22661.
32. Mugnaini E, Osen KK, Schnapp B, Friedrich VL Jr. (1977) Distribution of Schwann cell cytoplasm and plasmalemmal vesicles (caveolae) in peripheral myelin sheaths. An electron microscopic study with thin sections and freeze-fracturing. *J Neurocytol* 6:647–668.
33. Edgar JM, McCulloch MC, Thomson CE, Griffiths IR (2008) Distribution of mitochondria along small-diameter myelinated central nervous system axons. *J Neurosci Res* 86:2250–2257.
34. Dutta R, et al. (2006) Mitochondrial dysfunction as a cause of axonal degeneration in multiple sclerosis patients. *Ann Neurol* 59:478–489.
35. Hwang SI, et al. (2006) Systematic characterization of nuclear proteome during apoptosis: a quantitative proteomic study by differential extraction and stable isotope labeling. *Mol Cell Proteomics* 5:1131–1145.